M7-011 Effect of Different Shaft Orientation Due to Stability of Anisotropic Rotor

Jhon Malta

Department of Mechanical Engineering, Faculty of Engineering, Andalas University
Kampus Limau Manis, Padang 25163, Indonesia
Phone: +62-751-72586, Fax: +62-751-72566
E-mail: jhonmalta@ft.unand.ac.id

ABSTRACT

This research deals with a new discrete model of anisotropic rotor. In case of an anisotropic rotor has the difference in the shaft orientation, in which the direction of the principal axis of the shaft cross-section in the left shaft end is different from the direction in the right shaft end. In order to simplify the developed model, the rotor is supported by rigid bearings. The effect of the gyroscopic moments must be taken into account, whether a rigid disk is attached symmetry or asymmetry on the shaft. The sources of the gyroscopic moments in the system are distinguished into two types. In the first type, the occurrence of the gyroscopic moments in the system is caused by the difference in the shaft orientation. In the second type, it is caused by the asymmetric position of a rigid disk on the shaft. The effects of the gyroscopic moments which come from the difference in the shaft orientation and the asymmetry position of the disk on the shaft have the different characteristics due to the stability of the anisotropic rotor. The stability chart of the rotor is considered through analysis of eigenvalues of the system. For purely anisotropic rotor, the stability chart of the model shows that the location of the unstable area lies exactly in the range between the first and the second natural frequencies. By increasing the element anisotropy, the range of the instability becomes wider. For anisotropic rotor with the difference in the shaft orientation, the occurrence of the gyroscopic moments in the system is not significant or very small, but it contributes to the reduction of the interval of rotor instability.

Keywords: anisotropic rotor, shaft orientation, stability

1. Introduction

In case of a purely anisotropic rotor, the shaft stiffness of the rotor is different in the vertical and horizontal directions. In this case, the phenomenon of the weight critical occurs during the rotating anisotropic rotor and it has been examined by many researchers [1]. The fundamental theoretical investigations of an anisotropic rotor and its corresponding differential equations of motion have been studied by Kellenberger [2] and Ariaratnam [3]. In order to describe its basic characteristic, Michatz [4] investigated a simple Jeffcott rotor model, in which the effects of external and internal damping on the rotor have been taken into account. In this model, the instability of the rotor can be described accurately. Yamamoto et al [5] investigated an asymmetrical rotor with inequality in stiffness (i.e. different cross-sections along the shaft) including the effects of gyroscopic moments. However, the directions of the principal axes of the cross-sections are uniform. In case of an anisotropic rotor with a constant cross-section along the shaft (i.e. a purely anisotropic rotor), the system can be still approached by a Jeffcott rotor model, although its cross-section is placed not in the principal axis of the cross-section as presented in [6].

If a real rotor with different cross-sections along the shaft is modelled by discrete elements, it is possible that the elements will have different orientations of principal axes. In this paper, an anisotropic rotor with the difference in the shaft orientation is investigated. The direction of the principal axis of the shaft cross-section in the left shaft end is different from the direction in the right shaft end. In this condition, the Jeffcott rotor is no longer a satisfactory model. Therefore, a new discrete model must be developed. In order to simplify the developed model, the rotor is supported by rigid bearings. Nevertheless, the effect of the gyroscopic moments must be taken into account, whether a rigid disk is attached symmetry or asymmetry on the shaft. The sources of the gyroscopic moments in the system are distinguished into two types. In the first type, the occurrence of the gyroscopic moments in the system is caused by the difference in the shaft orientation. In the second type, it is caused by the asymmetric position of a rigid disk on the shaft. The effects of the gyroscopic moments which come from the difference in the shaft orientation and the asymmetry position of the disk on the shaft will be studied.

2. System Modelling

In Figure 1, the rotor shaft is modelled by two discrete elements which have different orientations of the principal axes of the element cross-sections. The rotor is simply supported by two rigid bearings. In order to simplify the shaft anisotropy, a rectangular cross section of the shaft is used. The anisotropies of all shaft elements are the same. By using the minimal number of elements, the rotor is discretized into two elements with the length ℓ_1 and ℓ_2, respectively. Therefore, the mathematical model can be simplified and possesses only four degrees of freedom, where the vibration of the shaft comes from only the motions ($\zeta_W, \eta_W, \varphi_\zeta, \varphi_\eta$) of the disk. The disk is assumed to be a thin disk with a ratio between polar mass and axial mass moment of inertia of 1.98 (i.e. disk radius = 0.06 m, disk thickness = 0.01 m). In the whole system, the internal and external dampings are neglected. As a point of interest, although the disk is attached symmetrically on the shaft ($\ell_1 = \ell_2$) and all elements have the same cross-sectional moment of inertia, but because of different orientation between the shaft elements, the disk position makes a precession. In this case, the effect of gyroscopic moments is no longer negligible.

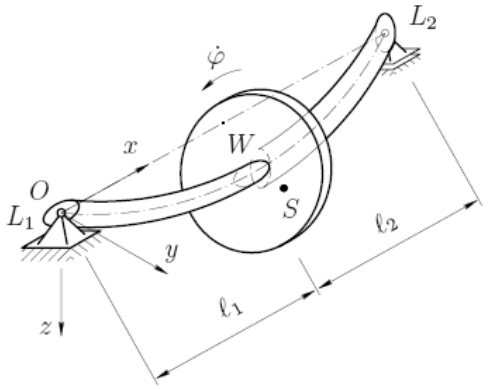

Figure 1 Anisotropic rotor with difference shaft orientation supported by rigid bearings

Based on the Fig. 2, if the rotor is assumed that has the minimal number of discrete elements (i.e. shaft with two elements only) the subscribe *k* has a value 1 or 2.

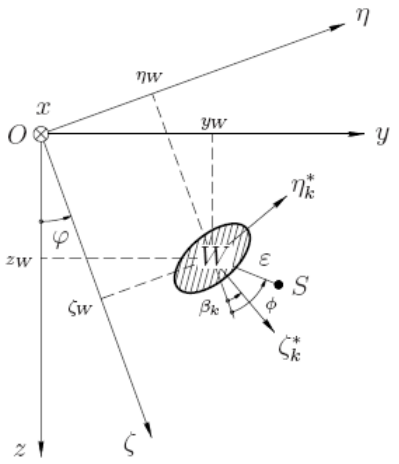

Figure 2 Coordinate system of anisotropic rotor

Furthermore, the coordinate systems of the principal axes of the first and the second shaft element are placed on the η_1^* - ζ_1^* - plane inclined at an angle β_1 and the η_2^* - ζ_2^* - plane at angle β_2. The centre of gravity *S* of the disk is eccentric to the centre of the shaft *W* and its position being defined by the eccentricity ε and the angular position ϕ. The kinematics relationships between the centre of gravity and the centre of shaft are

$$\begin{aligned} z_S &= z_W + \varepsilon\cos(\varphi+\phi) \\ y_S &= y_W + \varepsilon\sin(\varphi+\phi) \end{aligned} \qquad (1)$$

The kinematics relationships between coordinates of principal axes and rotating reference frame of the k^{th}-shaft element can be determined by using the following transformation equations

$$\begin{aligned}\zeta_k &= \zeta_k^* \cos\beta_k - \eta_k^* \sin\beta_k \\ \eta_k &= \zeta_k^* \sin\beta_k + \eta_k^* \cos\beta_k\end{aligned} \qquad (2)$$

and between rotating and fixed reference frames can be determined by using transformation equations as follows

$$\begin{aligned}z &= \zeta\cos\varphi - \eta\sin\varphi \\ y &= \zeta\sin\varphi + \eta\cos\varphi\ .\end{aligned} \qquad (3)$$

If a force acts on the rotor in arbitrary direction then this force is projected as F_ζ in ζ-direction and as F_ζ in η-direction. Furthermore, because of different shaft orientations, the force F_ζ is projected again on the first element to $F_{\zeta_1^*}$ and $F_{\eta_1^*}$ and on the second element to $F_{\zeta_2^*}$ and $F_{\eta_2^*}$. In the same way, the force F_η is projected on the first element to $F_{\zeta_1^*}$ and $F_{\eta_1^*}$ and is projected on the second element to $F_{\zeta_2^*}$ and $F_{\eta_2^*}$. Furthermore, if the resultant of forces in ζ_1^*-direction or ζ_2^*-direction has a positive value, then bending moment $M_{1\eta}^*$ or $M_{2\eta}^*$ will have a positive value. On the contrary, if resultant of forces in η_1^*-direction or η_2^*-direction has a positive value, then bending moment $M_{1\zeta}^*$ or $M_{2\zeta}^*$ will have negative value. In a moment diagram, the bending moments can be depicted as shown in Fig. 3.

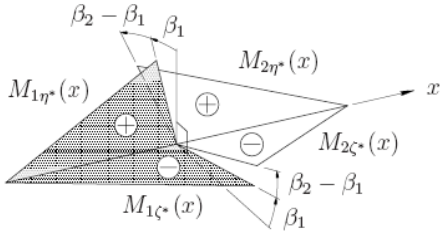

Figure 3 Bending moments in anisotropic rotor with different shaft orientation

In order to simplify the mathematical model, the moments of inertia of cross-section in principal axes of shaft elements should be transformed to rotating reference frame by using the following equations

$$\begin{aligned}I_{k\zeta} = \int \eta_k^2\, dA &= \tfrac{1}{2}\left(I_{k\eta^*} + I_{k\zeta^*}\right) - \tfrac{1}{2}\left(I_{k\eta^*} - I_{k\zeta^*}\right)\cos 2\beta_k \\ &\quad - I_{k\eta^*\zeta^*}\sin 2\beta_k \end{aligned} \qquad (4a)$$

$$\begin{aligned}I_{k\eta} = \int \zeta_k^2\, dA &= \tfrac{1}{2}\left(I_{k\eta^*} + I_{k\zeta^*}\right) + \tfrac{1}{2}\left(I_{k\eta^*} - I_{k\zeta^*}\right)\cos 2\beta_k \\ &\quad + I_{k\eta^*\zeta^*}\sin 2\beta_k \end{aligned} \qquad (4b)$$

$$\begin{aligned}I_{k\eta\zeta} = -\int \eta_k\zeta_k\, dA &= -\tfrac{1}{2}\left(I_{k\eta^*} - I_{k\zeta^*}\right)\sin 2\beta_k \\ &\quad + I_{k\eta^*\zeta^*}\cos 2\beta_k \end{aligned} \qquad (4c)$$

3. Gyroscopic Moments

The differential equations of anisotropic rotor supported by rigid bearings have been formulated in the previous research [7]. As shown in Figure 4, the disk on the shaft is described in the coordinate system (*x'*, *y'*, *z'*), where the plane of disk is parallel to the *y'*-*z'*-plane. The *x'*-axis is perpendicular to that plane. Furthermore, *y'*-axis can move only in the *x*-*y*-plane and *z'*-axis in the *x*-*z*-plane, therefore y'-axis and z'-axis can be not-perpendicular, where their position can make precessions φ_z and φ_y, respectively. This means the coordinate system (*x'*, *y'*, *z'*) is no longer orthonormal.

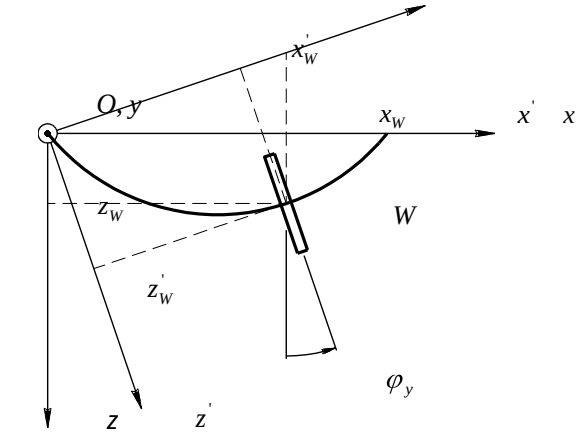

(a)

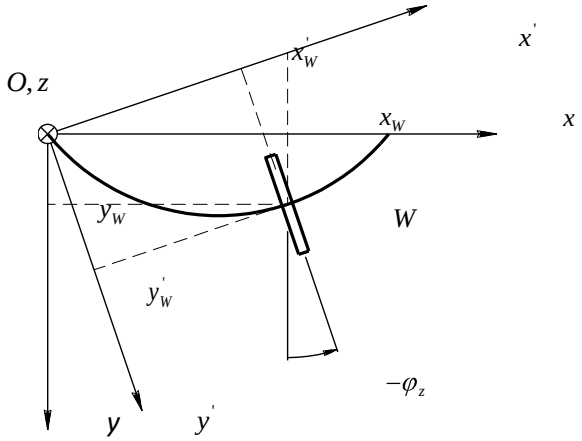

(b)

Figure 4 Coordinate of disk in anisotropic rotor system

From the Figure 4, the transformation equations of basis vectors are obtained

$$\begin{aligned}
\vec{e}_{z'} &= \sin\varphi_y\,\vec{e}_x + \cos\varphi_y\,\vec{e}_z \\
\vec{e}_{y'} &= -\sin\varphi_z\,\vec{e}_x + \cos\varphi_z\,\vec{e}_z \\
\vec{e}_{x'} &= \frac{\vec{e}_{y'}\times\vec{e}_z{}'}{\left|\vec{e}_{y'}\times\vec{e}_z{}'\right|} = \frac{\vec{e}_x + \tan\varphi_z\,\vec{e}_y - \tan\varphi_y\,\vec{e}_z}{\sqrt{1+\tan^2\varphi_y+\tan^2\varphi_z}}\,.
\end{aligned} \qquad (5)$$

Further, the kinematics relationships of angular velocities in (*x'*, *y'*, *z'*)-coordinate system are determined. If angular speed of the disk is denoted by ω_S in the (*x'*, *y'*, *z'*)-coordinate system, the *y'*-*z'*-plane that rotates along the *x'*-axis is denoted by ω_E and $\dot{\varphi}$ is the rotational speed of the shaft, then

$$\omega_S = \omega_E - \dot{\varphi}\,\vec{e}_{x'} \,. \qquad (6)$$

Furthermore, angular speed of basis vectors $\vec{e}_{y'}$ and $\vec{e}_{z'}$ are

$$\omega_{(y')} = \dot{\varphi}_{x'}\,\vec{e}_{x'} + \dot{\varphi}_{y'}\,\vec{e}_{y'} + \dot{\varphi}_{z'}\,\vec{e}_{z'} \qquad (7)$$

and

$$\omega_{(z')} = \dot{\varphi}_{x'}\,\vec{e}_{x'} + \dot{\varphi}_{y'}\,\vec{e}_{y'} + \dot{\varphi}_{z'}\,\vec{e}_{z'}, \qquad (8)$$

respectively. Note that, the expression in parenthesis is not a function argument but an alternative index. For an example, the $\dot{\varphi}_{x'}\,\vec{e}_{x'}$ means the rotational speed of the vector $\vec{e}_{x'}$ due to *y'*-axis. Because the plane of disk is placed at the *y'*-*z'*-plane and the precession φ_z is the angle of the plane of disk with respect to the *z*-axis, hence

$$\omega_{(y')} = \dot{\varphi}_z\,\vec{e}_z \,. \qquad (9)$$

Similar to the Eq. (9), the precession φ_y is the angle of the plane of disk with respect to the *y*-axis, hence

$$\omega_{(z')} = \dot{\varphi}_y\,\vec{e}_y \,. \qquad (10)$$

By using the Cramer's rule, angular speed $\dot{\varphi}_{x'}\,\vec{e}_{y'}$, $\dot{\varphi}_{y'}\,\vec{e}_{y'}$, $\dot{\varphi}_{z'}\,\vec{e}_{y'}$, $\dot{\varphi}_{x'}\,\vec{e}_{z'}$, $\dot{\varphi}_{y'}\,\vec{e}_{z'}$ and $\dot{\varphi}_{z'}\,\vec{e}_{z'}$ of the basis vectors can be determined. Based on the Figure 3, it is clear that the angular speed of the *y'*-*z'*-plane is the rotational speed of the vector $\vec{e}_{y'}$ due to *z'*-axis and the rotational speed of the vector $\vec{e}_{z'}$ due to *y'*-axis, hence the angular speed in Eq. (6) can be reformulated as

$$\omega_E = \dot{\varphi}_{y'}\,\vec{e}_{z'} + \dot{\varphi}_{z'}\,\vec{e}_{y'} \,. \qquad (11)$$

By inserting the basis vectors of the results of the Cramer's rule and the Eq. (11) into the Eq. (6), the ω_S can be reformulated. Furthermore, the vector of angular momentum can be calculated

$$L = \Theta\,\omega_S \,. \qquad (12)$$

If the precessions φ_z and φ_y are assumed to be small then

$$L = (\Theta_p \dot{\varphi})\,\vec{e}_x + (\Theta_p \dot{\varphi}\varphi_z + \Theta_a \dot{\varphi}_y)\,\vec{e}_y + (\Theta_p \dot{\varphi}\varphi_y + \Theta_a \dot{\varphi}_z)\,\vec{e}_z \,. \qquad (13)$$

The time derivative of angular momentum in rotating reference frame can be rewritten as

$$\frac{dL}{dt} = \left(\Theta_p \ddot{\varphi}\right)\vec{e}_x + \left[\Theta_p\left(\ddot{\varphi}\varphi_\eta + \dot{\varphi}^2\varphi_\zeta + \dot{\varphi}\dot{\varphi}_\eta\right) + \Theta_a\left(\ddot{\varphi}_\zeta - \dot{\varphi}^2\varphi_\zeta - 2\dot{\varphi}\dot{\varphi}_\eta - \ddot{\varphi}\varphi_\eta\right)\right]\vec{e}_\zeta + \left[\Theta_p\left(\ddot{\varphi}\varphi_\zeta + \dot{\varphi}^2\varphi_\eta - \dot{\varphi}\dot{\varphi}_\zeta\right) + \Theta_a\left(\ddot{\varphi}_\eta - \dot{\varphi}^2\varphi_\eta + 2\dot{\varphi}\dot{\varphi}_\zeta + \ddot{\varphi}\varphi_\zeta\right)\right]\vec{e}_\eta \qquad (14)$$

4. Differential Equations of Motion

The anisotropic rotor is modelled in rotating reference frame. Therefore, the rotor system becomes speed-dependent. The stability chart of the rotor is considered through analysis of eigenvalues of the system. In the developed model, the shaft stiffness matrix is assembled in the rotating reference frame by considering asymmetric bending by means of the strain energy method. In this paper, the formulation of the strain energy in asymmetric bending is not presented. For further information, this formulation can be found in [8] and [9].

The shaft is assumed to be massless, because the shaft mass is very light compared to the rotor mass. By using the minimal number of discrete elements, the size of the shaft stiffness matrix can be minimalized. For an anisotropic rotor with single disk, the shaft is discretized by two elements only. The flexibility influence coefficients (h_{ij}) of the shaft are obtained as follows

$$h_{ij} = \sum_{k=1}^{2} \int_{\ell_k} \frac{I_{k\zeta}}{E\left(I_{k\eta}I_{k\zeta} - I_{k\eta\zeta}^2\right)} \hat{M}_{ik\eta}\left(x\right)\hat{M}_{jk\eta}\left(x\right)dx \quad (15a)$$

for $i = 1,4$ and $j = 1,4$

$$h_{ij} = \sum_{k=1}^{2} \int_{\ell_k} \frac{I_{k\eta}}{E\left(I_{k\eta}I_{k\zeta} - I_{k\eta\zeta}^2\right)} \hat{M}_{ik\zeta}\left(x\right)\hat{M}_{jk\zeta}\left(x\right)dx \quad (15b)$$

for $i = 2,3$ and $j = 2,3$

$$h_{ij} = \sum_{k=1}^{2} \int_{\ell_k} \frac{-I_{k\zeta}}{E\left(I_{k\eta}I_{k\zeta} - I_{k\eta\zeta}^2\right)} \hat{M}_{ik\eta}\left(x\right)\hat{M}_{jk\zeta}\left(x\right)dx \quad (15c)$$

for $i = 1,4$ and $j = 2,3$

where E is the Young's modulus of the shaft material, ℓ_k is the length of shaft element and $\hat{M}$ is normalized moment bending. The flexibility matrix can be obtained by assembling these flexibility influence coefficients. The stiffness matrix is determined by inversion of the flexibility matrix.

Furthermore, the differential equations of translatory inertia (i.e. in the ζ and η-directions) in the rotating coordinate system can be determined by using 2nd Newton's Law, hence

$$m\left(\ddot{\zeta}_S - \ddot{\varphi}\eta_S - 2\dot{\varphi}\dot{\eta}_S - \dot{\varphi}^2\zeta_S\right)\vec{e}_\zeta + m\left(\ddot{\eta}_S + \ddot{\varphi}\zeta_S + 2\dot{\varphi}\dot{\zeta}_S - \dot{\varphi}^2\eta_S\right)\vec{e}_\eta = \sum_n F_n . \qquad (16)$$

Note that, the Eq. (16) is still defined in the centre of gravity of the disk. The differential equations of rotary inertia (i.e. in the φ_ζ and φ_η-directions) can be obtained by using the formulations in the Eq. (14) and the stiffness matrix especially in the φ_ζ and φ_η-directions.

In general, the differential equations of motion of the rotor can be witten as

$$[M]\{\ddot{q}\} + [D]\{\dot{q}\} + [C]\{q\} = \{F\} \qquad (17)$$

where $[D]$ and $[C]$ are speed-dependent proportional matrices due to velocity and displacement, respectively.

5. Stability Investigation

The stability of the rotor system is considered based on the homogenous linear equations of motion of the rotor in the Eq. (17), hence

$$[M]\{\ddot{q}\} + [D]\{\dot{q}\} + [C]\{q\} = \{0\}. \qquad (18)$$

This equation can be rearranged in state-space in order to reduce the differential equations to first-order.

$$\begin{bmatrix} [D] & [C] \\ [C] & [0] \end{bmatrix} \begin{Bmatrix} \{\dot{q}\} \\ \{q\} \end{Bmatrix} - \begin{bmatrix} [-M] & [0] \\ [0] & [C] \end{bmatrix} \begin{Bmatrix} \{\dot{q}\} \\ \{q\} \end{Bmatrix} = \begin{Bmatrix} \{0\} \\ \{0\} \end{Bmatrix} \qquad (19)$$

For simplification in writing, the Eq. (19) can be written as

$$[A]\{\dot{x}\} + [B]\{x\} = \{0\}. \qquad (20)$$

By solving the Eq. (20), the eigenvalues and eigenvectors can be considered. The eigenvector in this solution is usually called as right eigenvectors. In stability analysis, the solution of eigenvalues according to Eq. (20) is already sufficient. Usually, the eigenvalues are complex frequencies consisting of a real part (i.e. defined as decay rate, where it decreases amplitude in time) and an imaginary part (i.e. natural frequencies). An instability condition is involved if at least one of the real parts of the eigenvalues is positive value.

6. Case study and Discussion

As depicted in Fig. 1, the rotor shaft is modelled by two discrete elements which have different orientations of the principal axes of the element cross sections. The rotor is simply supported by two rigid bearings. In order to simplify the shaft anisotropy, a rectangular cross section of the shaft is used. The anisotropies of all shaft elements are the same and are defined as

$$\mu_W = \left| \frac{I_{\zeta^*} - I_{\eta^*}}{I_{\zeta^*} + I_{\eta^*}} \right|. \qquad (21)$$

In the numerical simulation, the coefficient μ_W of the element anisotropy is varied from 0 to 0.99. The width of the rectangular cross section is defined to be constant (e.g. $b = 8$ mm) and the thickness h of the cross section is formulated as

$$h = b\sqrt{\frac{1-\mu_W}{1+\mu_W}} \qquad (22)$$

A rigid disk is also attached on the shaft at the distance ℓ_1 from the left shaft end or ℓ_2 from the right shaft end. The disk is assumed to be a thin disk with a ratio between polar mass and axial mass moment of inertia of 1.98 (i.e. disk radius = 0.06 m, disk thickness = 0.01 m). In the whole system, the internal and external dampings are neglected.

Furthermore, four cases of anisotropic rotors are discussed in this section. First, the simulation of a purely anisotropic rotor ($\Delta\beta = 0$) supported by rigid bearings is performed. A disk is attached in the centre of the shaft. Similar to the investigation above, the model is analyzed to obtain the characteristics of stability through eigenvalue analyses of anisotropic rotor without gyroscopic moments acting on the system. In the other models, the effects of gyroscopic moments are taken into account. These effects are also distinguished into two types. In the first type, the disk is not attached in the centre of the shaft and the gyroscopic moments come only from the asymmetry of the rotor. This is simulated in Model 2. In the second type, the gyroscopic moments come only from the difference in the shaft orientation as simulated in Model 3. Finally, both sources of the gyroscopic moments from the asymmetry of the rotor and the difference in the shaft orientation are taken into account in Model 4. The parameters of the four rotor cases are listed in Table 1.

In case of the purely anisotropic rotor, the instability area as depicted in Fig. 5 lies exactly in the range between the first and the second natural frequency of the anisotropic rotor. The coefficient of the element anisotropy is varied between $\mu_W = 0$ and 0.99. At each coefficient of the element anisotropy, the first and the second natural frequencies are considered as the forward whirl speeds at rotational speed $\Omega = 0$. These natural frequencies have been normalized by the first natural frequency. Because of purely anisotropic along the rotor shaft, the first and second natural frequencies of the rotor correspond to the mode of U-form of the shaft bending in each direction of shaft cross-section. At the third and the fourth natural frequencies the rotor modes have S-form of the shaft bending and no instability exists. The instability area depicted in Fig. 5 is equivalent to the case of a purely anisotropic rotor investigated in [1] or [10].

Table 1 Parameter of rotor cases

Model	ℓ_1 [m]	ℓ_2 [m]	β_1 [^{o}]	β_2 [^{o}]	Chart
1	0.25	0.25	0	0	Fig.5
2	0.10	0.40	0	0	Fig.6
3	0.25	0.25	0	30	Fig.7
4	0.10	0.40	0	30	Fig.8

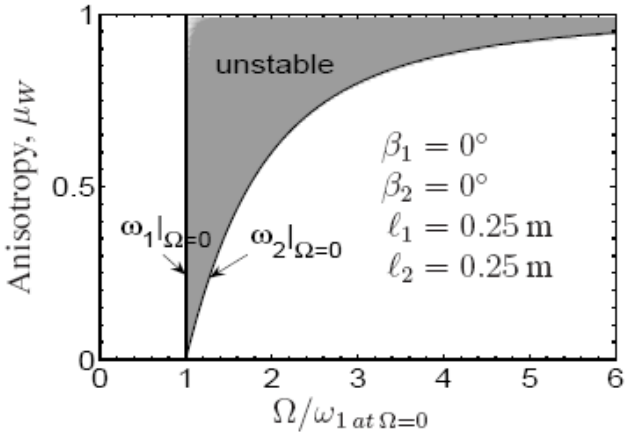

Figure 5 Stability chart of undamped anisotropic rotor (Model 1)

In Fig. 6, the instability area of the Model 2 is presented. In this model, the position of the disk is asymmetric on the shaft and the rotor is purely anisotropic. Therefore, the significant gyroscopic moments will occur in the system. The increase of gyroscopic moments cause the stiffness of the rotor stiffer and the instability range is wider.

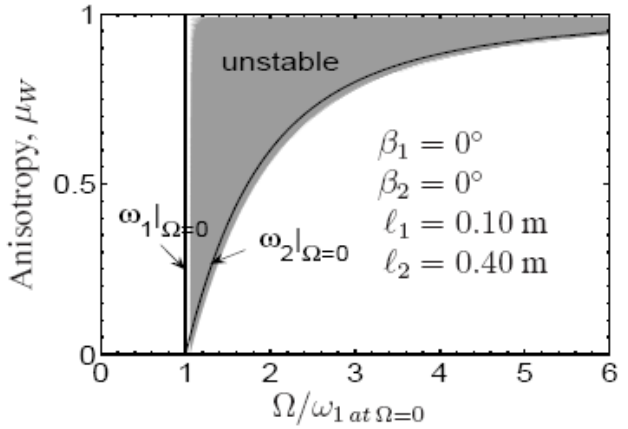

Figure 6 Stability chart of undamped anisotropic rotor (Model 2)

In Model 3, the anisotropic rotor with a thin disk attached symmetrically ($\ell_1 = \ell_2 = 0.25\,\mathrm{m}$) on the shaft has different shaft orientation $\beta_1 = 0°$ and $\beta_1 = 30°$ and the instability area of the model is plotted in Fig. 7. In this case, the inclination of the disk will not be equal to zero. Therefore, the gyroscopic moments still occur in the system, although they are negligible especially for lower values of μ_W. For further investigation, it is observed that the higher the coefficient of the element anisotropy of the shaft, the higher is the shift of the instability area to higher frequencies due to the first and the second natural frequencies. Nevertheless, the difference in the shaft orientation affects the reduction of the interval of the instability range.

The case of an anisotropic rotor with the disk located asymmetrically on the shaft $\ell_1 \neq \ell_2$ together with the difference $\beta_1 = 30^o$ in the shaft orientation is described in Model 4. The instability area of this model is presented in Fig. 8. The parameters of the asymmetry position of the disk and the difference in the shaft orientation show the same effect in shifting the instability area to higher frequencies but a contrary effect in reduction the width of instability. While the asymmetric rotor increases, the difference in the shaft orientation decreases the width of instability.

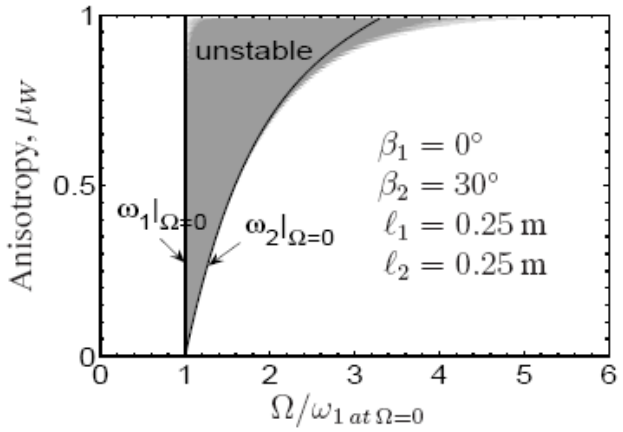

Figure 7 Stability chart of undamped anisotropic rotor (Model 3)

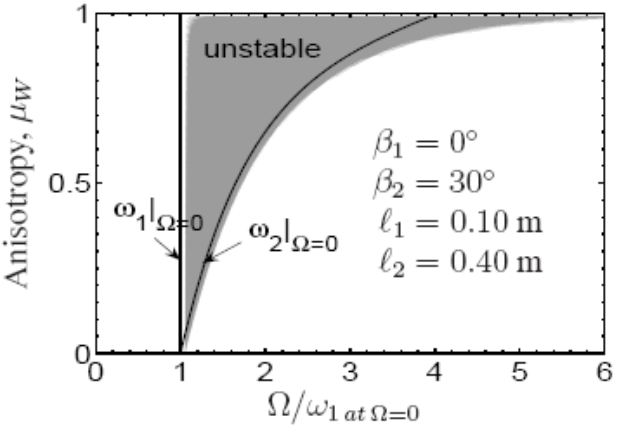

Figure 8 Stability chart of undamped anisotropic rotor (Model 4)

7. Conclusions

In the present investigation, a new model of anisotropic rotor with different shaft orientation has been developed. The gyroscopic moments are taken into account. The stability chart of the model shows that the location of the unstable area lies exactly in the range between the first and the second natural frequencies. By increasing the element anisotropy, the range of the instability becomes wider. By the difference in the shaft orientation in the rotor, the occurrence of the gyroscopic moments in the

system is not significant or very small, but it contributes to the reduction of the interval of rotor instability. The bigger the difference in the shaft orientation $\Delta\beta$, the narrower is the range of the instability area. The effect of the gyroscopic moments occurs significantly if the disk position is asymmetric on the shaft. An increase in the gyroscopic moments causes the rotor to become stiffer and the instability range wider.

References

[1] Gasch, R., Nordmann, R. and Pfützner, H., *Rotordynamik*, 2. Auflage, Ed. Berlin, Germany: Springer-Verlag, 2006.
[2] Kellenberger, *Biegeschwingungen einer unrunden, rotierenden Welle in horizontaler Lage*, Ingenieur-Archiv 26, 1958, pp. 302-318.
[3] Ariaratnam, S. T., *The Vibration of Unsymmetrical Rotating Shafts*, Journal of Applied Mechanics, Transactions of ASME, Mar. 1965, pp. 157-162.
[4] Michatz, J., *Das Biegeverhalten einer einfach besetzten, unrunden rotierenden Welle unter Berücksichtigung äußerer und innerer Dämpfungeinflüsse*, Dissertation an der TU Berlin, 1970.
[5] Yamamoto, T., Ota, H., Kono, K., On *the Unstable Vibrations of a Shaft with Unsymmetrical Stiffness Carrying an Unsymmetrical rotor*, Journal of Applied Mechanics, 35 (1968), pp. 313-321.
[6] Malta, J., On *the dynamics of flexible anisotropic rotor*, Proc. of ISSM, TU Delft, the Netherlands, 2008, pp. 243-247.
[7] Walter, F., *Bewegungsdifferentialgleichungen für das Auf- und Abfahren einer Laval-Welle*, Diplomarbeit am 1. Institut für Mechanik der TU Berlin, 1978.
[8] Markert, R., *Technische Mechanik, Teil A und B*, Skript zur Vorlesung, 1. Auflage, TU Darmstadt, 2002.
[9] Krämer, E., *Maschinendynamik*, Berlin Heidelberg: Springer-Verlag, 1984.
[10] Teichmann, H., *Biegeschwingungsverhalten von unrunden Rotoren in Gleitlagern*, Dissertation an der TU Berlin, Verlag Shaker, Aachen, 1995.